Published in final edited form as:
Brain Res. 2014 March 25; 1555: 20–27. doi:10.1016/j.brainres.2014.01.033.

Functional MR imaging of a simulated balance task

Helmet T. Karim[a], **Patrick J. Sparto**[b,c,d], **Howard J. Aizenstein**[d,e], **Joseph M. Furman**[c,d], **Theodore J. Huppert**[a,d], **Kirk I. Erickson**[f], and **Patrick J. Loughlin**[d,*]

[a]University of Pittsburgh, Department of Radiology, USA

[b]University of Pittsburgh, Department of Physical Therapy, USA

[c]University of Pittsburgh, Department of Otolaryngology, USA

[d]University of Pittsburgh, Department of Bioengineering, USA

[e]University of Pittsburgh, Department of Psychiatry, USA

[f]University of Pittsburgh, Department of Psychology, USA

Abstract

Human postural control, which relies on information from vestibular, visual, and proprioceptive inputs, degrades with aging, and falls are the leading cause of injury in older adults. In the last decade, functional neuroimaging studies have been performed in order to gain a greater understanding of the supraspinal control of balance and walking. It is known that active balancing involves cortical and subcortical structures in the brain, but neuroimaging of the brain during these tasks has been limited. The study of the effect of aging on the functional neuroimaging of posture and gait has only recently been undertaken. In this study, an MRI-compatible force platform was developed to simulate active balance control. Eleven healthy participants (mean age 75 ± 5 yr) performed an active balance simulation task by using visual feedback to control anterior–posterior center of pressure movements generated by ankle dorsiflexor (DF) and plantarflexor (PF) movements, in a pattern consistent with upright stance control. An additional ankle DF/PF exertion task was performed. During both the active balance simulation and the ankle DF/PF tasks, the bilateral fusiform gyrus and middle temporal gyrus, right inferior, middle, and superior frontal gyrii were activated. No areas were found to be more active during the ankle DF/PF task when compared with the active balance simulation task. When compared to the ankle DF/PF task, the active balance simulation task elicited greater activation in the middle and superior temporal gyrii, insula, and a large cluster that covered the corpus callosum, superior and medial frontal gyrii, as well as the anterior cingulate and caudate nucleus. This study demonstrates the utility in using a force platform to simulate active balance control during MR imaging that elicits activity in cortical regions consistent with studies of active balance and mental imagery of balance.

Keywords

Balance; fMRI; Brain activation

*Corresponding author. loughlin@pitt.edu (P.J. Loughlin)..

1. Introduction

Maintaining upright balance and walking are two of the most fundamental activities performed by humans. In older adults (age 65 years and older) and people with movement disorders, the ability to stand upright and walk without falling is a significant contributor to the prevention of disability and to the maintenance of quality of life (Tinetti and Williams, 1998; Heesch et al., 2012). Balance deficits are a key contributor to falls, especially among older adults, where it is estimated that 1 in 3 experience a fall each year (Hausdorff et al., 2001). Falls are a leading cause of injury and even death, costing billions of dollars annually in medical costs and adversely affecting a person's function and quality of life (Davis et al., 2010; Stevens et al., 2006, 2008). Roughly 25% of those who fall suffer debilitating injuries that can lead to decreased independence and early admission to nursing homes (Sterling et al., 2001).

Despite the importance of balance and locomotion to one's overall function and well-being, our understanding of their cortical control is incomplete. In the last two decades, functional neuroimaging studies have been performed in order to gain a greater understanding of the supraspinal control of balance and walking. Tasks have included both active and mental imagery of stance, walking and running, as well as active and passive ankle movement, and ankle and knee torque production (Bakker et al., 2008). The majority of these studies have focused on imaging of walking (Bakker et al., 2007; Jahn and Zwergal, 2010). During these activities, cortical activation is widely distributed, and greatly task dependent.

Other studies have investigated the neuroanatomy of active balance control. Previous studies have utilized positron emission tomography (PET) (Ouchi et al., 1999; Malouin et al., 2003), functional magnetic resonance imaging (fMRI) (Jahn et al., 2004; Zwergal et al., 2012), and functional near-infrared spectroscopy (fNIRS) (Mihara et al., 2008) techniques to investigate cortical and subcortical structures involved in active balancing and mental imagery of balance. Although these studies have elucidated some of the regions that may be involved in true active balance, some were limited to mental imagery of balance (Malouin et al., 2003; Jahn et al., 2004; Zwergal et al., 2012). Mihara et al. performed active balancing but the examination was limited to superficial cortical structures in the frontal cortex as fNIRS was used (Mihara et al., 2008). Ouchi et al. investigated upright stance but used a PET system that limited subject movement and did not cover the primary somatosensory foot area (Ouchi et al., 1999). Despite this, these studies have provided important information regarding the roles of the cortex and deeper structures in human postural control.

These studies have found that frontal areas such as the dorsolateral prefrontal cortex, superior and inferior frontal gyrii, and precentral gyrus are involved in balancing (Ouchi et al. 1999; Malouin et al., 2003; Jahn et al., 2004; Mihara et al., 2008; Zwergal et al., 2012). Also, the parieto-insular vestibular cortex, superior and inferior temporal gyrii, inferior parietal lobe, anterior vermis, precuneus, and thalamus are also activated (Ouchi et al., 1999; Malouin et al., 2003; Jahn et al., 2004; Zwergal et al., 2012).

The study of the effect of aging on the functional neuroimaging of posture and gait has only recently been undertaken (Zwergal et al., 2012). Imagined standing elicited age-dependent

activation of cortical areas devoted to processing of sensory signals, including the bilateral insula, superior and middle temporal gyrus, inferior frontal gyrus, middle occipital gyrus and postcentral gyrus (Zwergal et al., 2012). These areas were more active in older adults during imagined standing compared with imagined walking and running, which is considered to reflect reduced reciprocal inhibition of these areas in older adults.

The purpose of this current study was to investigate brain regions involved in a simulated active balance task using functional MRI with an MRI-compatible force platform. The active balance task was performed while supine and consisted of isometric ankle dorsiflexor and plantarflexor force production that simulated the movement of center of pressure during upright balancing.

2. Results

The average RMS error in performance across all four of the active balance simulation tasks was 1.1 (SD 0.2) cm. The size of the error depended on the scan order (Friedman test $\chi^2(3)=13.4$, $p=0.004$), with a larger error during the first scan (1.3±0.4 cm) compared with the final 3 scans (1.0±0.3 cm, Wilcoxon signed ranks test, $p<0.05$).

A conjunction analysis was performed to identify parts of the brain that were activated during both the ankle DF/PF and active balance simulation tasks compared to the visual stimulation control task (Table 2). This analysis showed portions of the supplemental motor area within the right inferior frontal/precentral gyrii, right middle frontal gyrus and right superior frontal gyrus. Functional visual and visual processing areas such as the fusiform/middle temporal gyrii (BA 19/37) were activated bilaterally. To visualize these activations (effect sizes), they are projected onto six representative slices of a T2-weighted structural image (Fig. 3) as well as a 3D-rendered surface brain (Fig. 4). They show that the active balance simulation task and the ankle DF/PF task both have areas activated that are involved in visual, motor, and premotor function.

Analysis of contrast between the active balance simulation task and the ankle DF/PF task revealed that there were no areas that were significantly activated more during the ankle DF/PF task than the active balance simulation task. In contrast, the active balance simulation task elicited greater activation than the ankle DF/PF task in several regions (Table 3). These included frontal areas such as the left inferior frontal gyrus and a large cluster that covered the corpus callosum, superior and middle frontal gyrii, the caudate nucleus, and anterior cingulate. This suggests that the active balance simulation task may have had a more demanding cognitive component than the ankle DF/PF task. The middle temporal gyrus in the left and right hemisphere as well as the insula on the right hemisphere and superior temporal gyrus in the left hemisphere were also activated more for the active balance simulation task compared to the ankle DF/PF task. These regions are known for visual-vestibular and multisensory integration. These areas are shown across six different slices (Fig. 3) as well as a 3D-rendered surface of the brain (Fig. 4).

3. Discussion

In this study, an MRI-compatible force platform was developed and used to investigate cortical activation elicited during rhythmic ankle muscle contractions and a simulated balance task. The active balance simulation required ankle muscle activation patterns that produced changes in center of pressure movement consistent with quiet upright stance. This study augments previous work that has used imagined stance conditions during fMRI to gain insight into the neural control of upright balance.

Previously, several different methods, including brain lesion studies and neuroimaging, have been used to gain an understanding of the structures involved in upright balance. For example, patients with unilateral stroke in the parieto-temporal junction and parieto-insular vestibular cortex have poor static and dynamic balance (Perennou et al., 2000; Ustinova et al., 2001). The structures required for maintenance of standing posture in humans also have been investigated using functional near-infrared spectroscopy (fNIRS) (Mihara et al., 2008), positron emission tomography (PET) (Ouchi et al., 1999; Malouin et al., 2003), and functional magnetic resonance imaging (fMRI) (Jahn et al., 2004; Zwergal et al., 2012).

Some studies have used mental imagery of stance to infer which subcortical and cortical structures are used in actual stance, and have found widely distributed regions of activation that include areas of multisensory processing and integration, motor planning, and executive function. Malouin et al. using PET, found that mental imagery of stance produced activation in the inferior parietal lobe, dorsolateral prefrontal cortex, sensorimotor regions, the precuneus, and right posterior cingu-late (Malouin et al., 2003). Jahn et al. found that imagined stance using fMRI elicited activation in the thalamus, superior and inferior frontal gyrii, and middle temporal gyrus, cerebellar hemispheres and vermis, and basal ganglia (Jahn et al., 2004). Additional studies by the same group revealed activation of supplementary motor area, anterior cingulate gyrus, insula, supramarginal gyrus, and precuneus. An even more recent study by Zwergal et al. used fMRI to confirm the same regions were active in older adults as well as young adults (Zwergal et al., 2012). Another interesting study of imagined stance required subjects to view stable and unstable upright postures from a third-person perspective. Viewing of unstable postures resulted in activation of bilateral parietal lobe, anterior cingu-late cortex, and cerebellum (Slobounov et al., 2006).

Other studies have investigated activation during actual upright stance. Ouchi et al. used a mobile gantry H_2O PET system during different standing positions (e.g. feet together with eyes open and closed, and feet in tandem) (Ouchi et al., 1999). They found that the visual cortex, cerebellum, anterior vermis, and inferior temporal gyrus were involved in active balance conditions (Ouchi et al., 1999). A study by Mihara et al. used fNIRS, which is limited to cortical activation and not subcortical activation, and had subjects maintain stance on a platform that was perturbed (horizontally) forward and backwards (Mihara et al., 2008). They found that there were bilateral middle and superior frontal activation as well as right precentral gyrus activation (Mihara et al., 2008).

Our results using a novel MRI-compatible force platform to simulate active balance sensori-motor activity were consistent with many of these previous findings. A conjunction analysis

between the active balance simulation task and the ankle DF/PF task was performed, using a non-motor visual stimulation task as the control. Several regions of significantly increased BOLD signal were observed between both tasks, including the fusiform/middle temporal gyrus bilaterally, superior, middle and inferior frontal gyrii on the right, as well as the right precentral gyrus. Activation of the fusiform and middle temporal gyrii (Dupont et al., 1994; Beer et al., 2002; Deutschlander et al., 2002), and superior frontal gyrus (Inoue et al., 2000) is probably related to visual motion processing and visuo-motor learning. The middle and inferior frontal gyri play a role in executive function processes, in particular inhibition (Vollm et al., 2006; Picton et al., 2007) and error detection. The relationship between inhibitory control and balance performance has previously been established, specifically for sensory integration and balance performance (Redfern et al., 2009). The premotor and supplementary motor areas within the superior frontal gyrus were probably active because of their involvement in guiding movements based on visual feedback (Schubotz and von Cramon, 2002) and motor learning (Inoue et al., 2000).

An analysis of contrast between the active balance simulation task and the ankle DF/PF task did not detect any regions that were activated to a greater extent during the ankle DF/PF task compared with the active balance simulation task. However, there were several regions that were activated more in the active balance simulation task compared with the ankle DF/PF task. In particular, we observed a large cluster in the corpus callosum that extended into the superior and medial frontal gyrii, as well as the caudate body and anterior cingulate. It is likely that the active balance simulation task required a greater degree of attention and error detection in order to keep the pseudorandom target movement in the center, whereas the target placement during the ankle DF/PF task was deterministic. Also, we found areas such as the left middle temporal gyrus (BA 22), left superior temporal (BA 22) gyrus, and the right insula were also more active in the active balance simulation than the DF/PF task. These results indicate that the active balance simulation required greater activation in regions that are involved in visual-vestibular and multisensory integration (Hugdahl et al., 2006; Dieterich and Brandt, 2008).

3.1. Limitations

Although the smaller sample size of older subjects may limit the generalizability of the study, given the concordance with previous findings in the literature, the results appear to be robust. Nonetheless, additional studies with a larger cohort of older subjects are needed to confirm the findings. In addition, we acknowledge that the neural activation elicited by a task performed in supine may not completely represent the activation of standing upright balance. However, the results are reinforced by the PET and NIRS imaging studies that were performed during upright standing (Mihara et al., 2008; Ouchi et al., 1999).

4. Conclusion

These results demonstrate that the active balance simulation task using a force platform in the supine position can elicit activation similar to those seen in previous studies. Specifically, we found that visual, visual processing, and motor areas were activated in both the active balance simulation task and the ankle DF/PF task (or motor control). Furthermore,

we found that the active balance simulation elicited greater activation in areas that were not active in the ankle DF/PF task. These areas include parts of the frontal cortex, caudate, and anterior cingulate as well as the insula and middle/superior temporal gyrii suggesting that the active balance simulation task had a greater cognitive and sensory processing component.

5. Experimental procedures

5.1. Subject population

A total of 11 neurologically healthy, right-handed older adults (mean age 75±5 years, 7 female) participated after providing informed consent. Subjects underwent a comprehensive screening examination to exclude subjects with a history of neurological, cardiopulmonary, or orthopedic disease that would limit their mobility and balance function (e.g. stroke, Parkinson's disease, vestibular disease, multiple sclerosis, uncontrolled diabetes, uncontrolled hypertension, chronic obstructive pulmonary disease, significant peripheral neuropathy, significant vision loss, peripheral vestibulopathy, severe arthritis). In addition, subjects were excluded if they had impaired neurocognitive function as determined by a score more than 1.5 SDs below age-adjusted mean in the Repeatable Battery for the Assessment of Neuropsychological Status (RBANS, Pearson Education, San Antonio TX) (Randolph, et al., 1998). This study was approved by the University of Pittsburgh Institutional Review Board.

5.2. Force platform

An MRI-compatible force platform was constructed (Fig. 1). Two aluminum plates (Alloy 6061-T651, 46 cm × 46 cm × 1.3 cm) were fixed to a support constructed of aluminum rectangular tubes (Alloy 6105-T5, 37 mm × 37 mm, 80-20 Inc, Columbia City, IN), which attached to the sliding patient bed of the MRI scanner (Siemen's TIM TRIO), via machined aluminum inserts and nylon straps. In addition, the platform could be fit to each subject's height by using an adjustable sliding mechanism that had 84 cm of travel. Each plate was fixed to the support structure using 2 uni-axial load cells (Vishay Model 1042 Low Profile Aluminum Load Cell, Malvern, PA), located at the top half and the bottom half of each plate (23 cm distance between load cells in AP direction, 41 cm distance in ML direction). The electronic amplifier/indicators (Interface Model 9830, Scottsdale, AZ) for the load cells were located in the MR control room, and RS-232 cables transmitted the voltage signals via a shielded interface board between the scanner and control rooms. Voltage signals from the amplifiers were then transduced to a USB data acquisition device (National Instruments USB-6008), and acquired using custom written software (National Instruments Labview 8.2) on a laptop computer. Weights were placed at locations on the force platform so that a calibration of the axial force and center of pressure location could be obtained from the voltage output of the four load cells.

In order to simulate weight-bearing, elastic cords were used to apply a caudally-directed force to the subject via a torso vest and waist belt. The amount of axial loading was between 25% and 50% of the subject's body weight, adjusted to the subject's comfort. Head

movement was minimized during the experiment by placing pillows around the head within the head coil.

5.3. Functional task design

During MRI scanning, three tasks were performed (as illustrated in Fig. 2). Within a single MR scan sequence, each of the three tasks, which appeared in random order, was preceded by a rest block in which the subjects read the instructions for the next task. The duration of the active blocks were 30 s, and the rest blocks were 10 s. The entire scan sequence was repeated four times, resulting in four blocks of each task for a total of 12 active blocks. The tasks were generated in National Instruments Labview (version 8.2) and projected onto a flat screen placed at the head of the scanner. The subjects were able to view the screen via a mirror placed above their eyes.

5.4. Visual stimulation control task

This task was used as a control for activation of the visual system (Fig. 2, A1). A vertical bar appeared at the center of the display with a stationary cross at the midpoint. Subjects were instructed to look at the display while relaxing their legs.

5.5. Ankle dorsiflexor/plantarflexor (DF/PF) activation task

This task was used as a control for activation of the primary motor areas related to the ankle dorsiflexors (DF) and plan-tarflexors (PF) (Fig. 2, A2 and A3). A red square appeared alternately at the top and bottom of the vertical bar, remaining at each location for 5 s at a time (Fig. 2, A2). The location of the COP in the anterior–posterior direction (relative to the subject) was displayed as a cross that moved up (i.e. anterior to body) and down the screen. The subject was instructed to press with his toes in order to move the cross to the red square at the top, and to press with his heels to move the cross to the red square at the bottom.

5.6. Active balance simulation task

This task required subjects to activate the dorsiflexors and plantarflexors in a pattern consistent with upright stance. A stationary circle was placed at the midpoint of the vertical bar (Fig. 2, B1). In the absence of an applied force by the subject, a cross would move pseudorandomly up and down the vertical bar according to a sum of sines displacement that had the frequency characteristics of human postural sway. When force was applied by the subject, the cross represented the summation of the pseudorandom displacement and the location of the COP in the anterior–posterior direction. The subject was instructed to keep the cross within the circle, which required the subject to counteract the sum of sines perturbation by pressing with his toes or heels to move the cross up or down (Fig. 2, B2 and B3).

5.7. Data acquisition

MRI scanning was done on a 3T Siemens TRIO scanner using a 12-channel parallel receive head coil. GE-EPI BOLD (FA=90° TR=2000 ms; TE=29 ms) scans were collected with 38 axial slices (3.4 mm thickness) with a 3.4 mm × 3.4 mm in-plane resolution (64 × 64). A T2-weighted structural scan (FA=150°, TR=3000 ms, TE=101 ms) with voxel size 1.0 × 1.0 ×

1.0 mm^3 (matrix 224 × 256) was used to acquire 48 slices covering the whole brain, which was collected prior to the functional scans.

5.8. fMRI data analysis

All fMRI data were analyzed using statistical parametric mapping software SPM8 (Friston, 2007). Each functional volume in the series was first aligned to the first functional volume to correct for subject motion. Each scan was examined for movement artifact and standard motion correction algorithms were applied. The motion translation and rotation parameters for the subjects are summarized in Table 1. Despite movement of the lower body during this task, very little head motion was noted in the MRI scans. None of the subjects had to be excluded due to excessive head motion artifacts.

The individual's T2-weighted structural image was aligned to the time-aligned average of the functional series. The T2-weighted structural scan was then registered and normalized (Friston et al., 1995) to the Montreal Neurological Institute (MNI) reference brain. Finally, functional BOLD series were spatially smoothed using a 6 mm full-width at half-maximum (FWHM) isotropic Gaussian kernel.

A canonical general linear model (GLM) analysis was applied to preprocessed fMRI BOLD data (Friston et al., 1995). The preprocessed data was de-convolved using a boxcar regression model with a 1/128 s high-pass filter. Motion parameters obtained from the realignment of the functional time-series were used as covariates in the model. In a first-level statistical analysis, subject-level contrasts for the active balance simulation task vs. visual stimulation control, the ankle DF/PF task vs. visual stimulation control, and the active balance simulation task vs. ankle DF/PF task were calculated. These SPMs were entered into a group-level statistical analysis (Friston, 2007). A threshold adjustment method based on Monte-Carlo simulations correction was used with a voxelwise $p<0.005$ and a minimum cluster size of 33 voxels yielded an AlphaSim correction threshold of $p<0.05$. AlphaSim is a tool from the AFNI (Analysis for Functional NeuroImaging) program that is used to estimate the probability of getting Type I errors given certain scan parameters (Cox, 1996). Blood oxygen level dependent (BOLD) signal increases and decreases were calculated and considered significant at $p<0.05$, AlphaSim corrected.

5.9. Force plate center of pressure (COP) data analysis

For the active balance simulation task, the location of the sum-of-sines perturbation and the center of pressure in the AP direction were sampled at approximately 100 Hz. The summation of these two signals, i.e. the distance of the cross from the stationary circle in scaled units (cm), was computed as the error in performance. The root-mean-square (RMS) of the error signal was calculated for each scan.

Acknowledgments

The authors thank James Cook and Colleen Nable for their instrumental work in conducting the experiment. This research was supported by funding from the National Institutes of Health (P30 AG024827, P30 DC005205), including the Pittsburgh Claude D. Pepper Older Americans Independence Center (P30 AG024827).

REFERENCES

Bakker M, De Lange FP, Helmich RC, Scheeringa R, Bloem BR, Toni I. Cerebral correlates of motor imagery of normal and precision gait. Neuroimage. 2008; 41(3):998–1010. [PubMed: 18455930]

Bakker M, Verstappen CC, Bloem BR, Toni I. Recent advances in functional neuroimaging of gait. J. Neural Transm. 2007; 114(10):1323–1331. [PubMed: 17622483]

Beer J, Blakemore C, Previc FH, Liotti M. Areas of the human brain activated by ambient visual motion, indicating three kinds of self-movement. Exp. Brain Res. 2002; 143(1):78–88. [PubMed: 11907693]

Cox RW. AFNI: software for analysis and visualization of functional magnetic resonance neuroimages. Comput. Biomed. Res. 1996; 29(3):162–173. [PubMed: 8812068]

Davis JC, et al. International comparison of cost of falls in older adults living in the community: a systematic review. Osteoporos. Int. 2010; 21(8):1295–1306. [PubMed: 20195846]

Deutschlander A, Bense S, Stephan T, Schwaiger M, Brandt T, Dieterich M. Sensory system interactions during simultaneous vestibular and visual stimulation in PET. Hum. Brain Mapp. 2002; 16(2):92–103. [PubMed: 11954059]

Dieterich M, Brandt T. Functional brain imaging of peripheral and central vestibular disorders. Brain: J. Neurol. 2008; 131(Pt 10):2538–2552.

Dupont P, Orban GA, De Bruyn B, Verbruggen A, Mortelmans L. Many areas in the human brain respond to visual motion. J. Neurophysiol. 1994; 72(3):1420–1424. [PubMed: 7807222]

Friston, KJ. Statistical Parametric Mapping: the Analysis of Functional Brain Images. Academic; London: 2007.

Friston KJ, Holmes AP, Poline JB, Grasby PJ, Williams SC, Frackowiak RS, Turner R. Analysis of fMRI time-series revisited. Neuroimage. 1995; 2(1):45–53. [PubMed: 9343589]

Hausdorff J, Rios D, Edelber H. Gait variability and fall risk in community living older adults: a 1 year prospective study. Arch. Phys. Med. Rehabil. 2001; 82(8):10506.

Heesch KC, van Uffelen JG, van Gellecum YR, Brown WJ. Dose-response relationships between physical activity, walking and health-related quality of life in mid-age and older women. J. Epidemiol. Community Health. 2012; 66(8):670–677. [PubMed: 22544920]

Hugdahl K, Thomsen T, Ersland L. Sex differences in visuo-spatial processing: an fMRI study of mental rotation. Neuropsychologia. 2006; 44(9):1575–1583. [PubMed: 16678867]

Inoue K, Kawashima R, Satoh K, Kinomura S, Sugiura M, Goto R, Ito M, Fukuda H. A PET study of visuomotor learning under optical rotation. Neuroimage. 2000; 11(5 Pt 1):505–516. [PubMed: 10806036]

Jahn K, Deutschlander A, Stephan T, Strupp M, Wiesmann M, Brandt T. Brain activation patterns during imagined stance and locomotion in functional magnetic resonance imaging. Neuroimage. 2004; 22(4):1722–1731. [PubMed: 15275928]

Jahn K, Zwergal A. Imaging supraspinal locomotor control in balance disorders. Restor. Neurol. Neurosci. 2010; 28(1):105–114. [PubMed: 20086287]

Malouin F, Richards CL, Jackson PL, Dumas F, Doyon J. Brain activations during motor imagery of locomotor-related tasks: a PET study. Hum. Brain Mapp. 2003; 19(1):47–62. [PubMed: 12731103]

Mihara M, Miyai I, Hatakenaka M, Kubota K, Sakoda S. Role of the prefrontal cortex in human balance control. Neuroimage. 2008; 43(2):329–336. [PubMed: 18718542]

Ouchi Y, Okada H, Yoshikawa E, Nobezawa S, Futatsubashi M. Brain activation during maintenance of standing postures in humans. Brain: J. Neurol. 1999; 122:329–338.

Perennou DA, Leblond C, Amblard B, Micallef JP, Rouget E, Pelissier J. The polymodal sensory cortex is crucial for controlling lateral postural stability: evidence from stroke patients. Brain Res. Bull. 2000; 53(3):359–365. [PubMed: 11113593]

Picton TW, Stuss DT, Alexander MP, Shallice T, Binns MA, Gillingham S. Effects of focal frontal lesions on response inhibition. Cereb. Cortex. 2007; 17(4):826–838. [PubMed: 16699079]

Randolph C, Tierney MC, Mohr E, Chase TN. The Repeatable Battery for the Assessment of Neuropsychological Status (RBANS): preliminary clinical validity. J. Clin. Exp. Neuropsychol. 1998; 20(3):310–319. [PubMed: 9845158]

Redfern MS, Jennings JR, Mendelson D, Nebes RD. Perceptual inhibition is associated with sensory integration in standing postural control among older adults. J. Gerontol. Ser. B Psychol. Sci. Soc. Sci. 2009; 64(5):569–576. [PubMed: 19617457]

Schubotz RI, von Cramon DY. A blueprint for target motion: fMRI reveals perceived sequential complexity to modulate premotor cortex. Neuroimage. 2002; 16(4):920–935. [PubMed: 12202080]

Sterling D, OConnor J, Bonadies J. Geriatric falls: injury severity is high and disproportionate to mechanism. J. Trauma. 2001; 50:116–119. [PubMed: 11231681]

Stevens J, Corso P, Finkelstein E, Miller T. The costs of fatal and nonfatal falls among older adults. Inj. Prev. 2006; 12:2905.

Stevens J, et al. Self-reported falls and fall relatedinjuries among persons aged ≥65 years—United States, 2006. J. Saf. Res. 2008; 39(3):345–349.

Slobounov S, Wu T, Hallett M. Neural basis subserving the detection of postural instability: an fMRI study. Motor Control. 2006; 10(1):69–89. [PubMed: 16571908]

Tinetti ME, Williams CS. The effect of falls and fall injuries on functioning in community-dwelling older persons. J. Gerontol. A Biol. Sci. Med. Sci. 1998; 53(2):M112–M119. [PubMed: 9520917]

Ustinova KI, Chernikova LA, Ioffe ME, Sliva SS. Impairment of learning the voluntary control of posture in patients with cortical lesions of different locations: the cortical mechanisms of pose regulation. Neurosci. Behav. Physiol. 2001; 31(3):259–267. [PubMed: 11430569]

Vollm B, Richardson P, McKie S, Elliott R, Deakin JF, Anderson IM. Serotonergic modulation of neuronal responses to behavioural inhibition and reinforcing stimuli: an fMRI study in healthy volunteers. Eur. J. Neurosci. 2006; 23(2):552–560. [PubMed: 16420462]

Zwergal A, Linn J, Xiong G, Brandt T, Strupp M, Jahn K. Aging of human supraspinal locomotor and postural control in fMRI. Neurobiol. Aging. 2012; 33(6):1073–1084. [PubMed: 21051105]

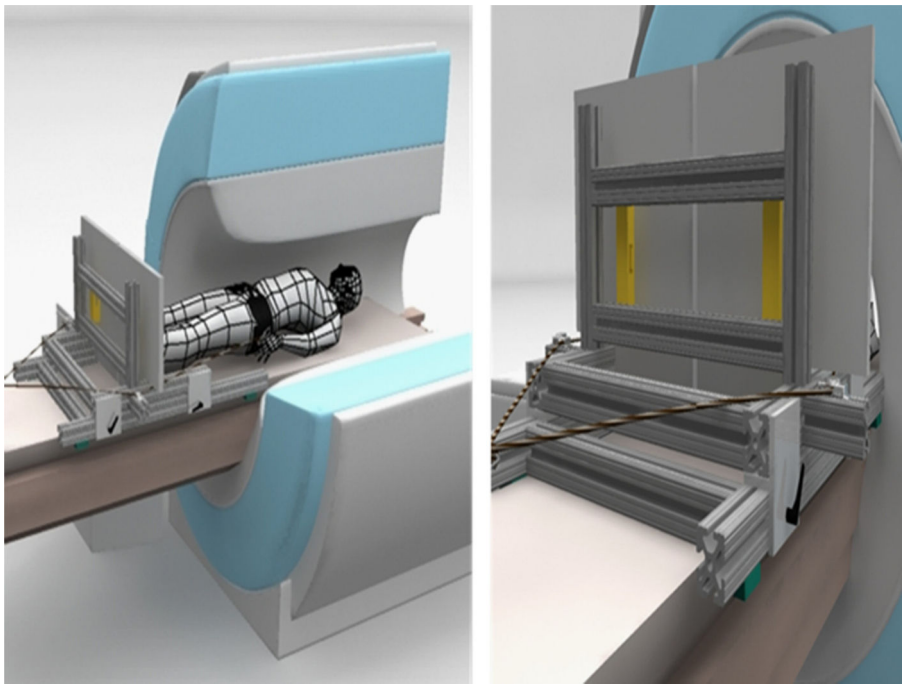

Fig. 1.

Schematic of MR-compatible posture platform. Left figure shows cut-away view of MR scanner with subject lying supine with feet against independently instrumented platforms. An axial compressive force between the subject and plate is applied via a belt around subject's waist. In view on right, axial load cells (shown in gold) can be seen between platforms and vertical supports.

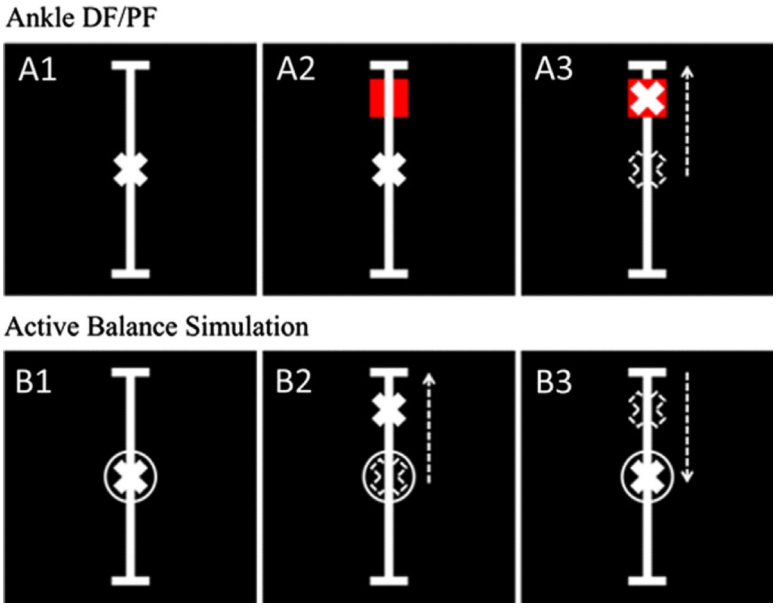

Fig. 2.

The visual stimulation control was defined as panel A1. The A2 and A3 panels describe the ankle DF/PF task in which subjects were asked to do a simple ankle dorsiflexion (DF) or plantarflexion (PF) to move a cross hair into a red square. The B panels describe the active balance simulation task in which the cross hair represented a summation of an unpredictable sum of sines perturbation with a frequency similar to that of human postural plus the center of pressure of the subject. The subjects were instructed to counteract the sum of sines perturbation using ankle DF/PF and keep the cross hair in the circle.

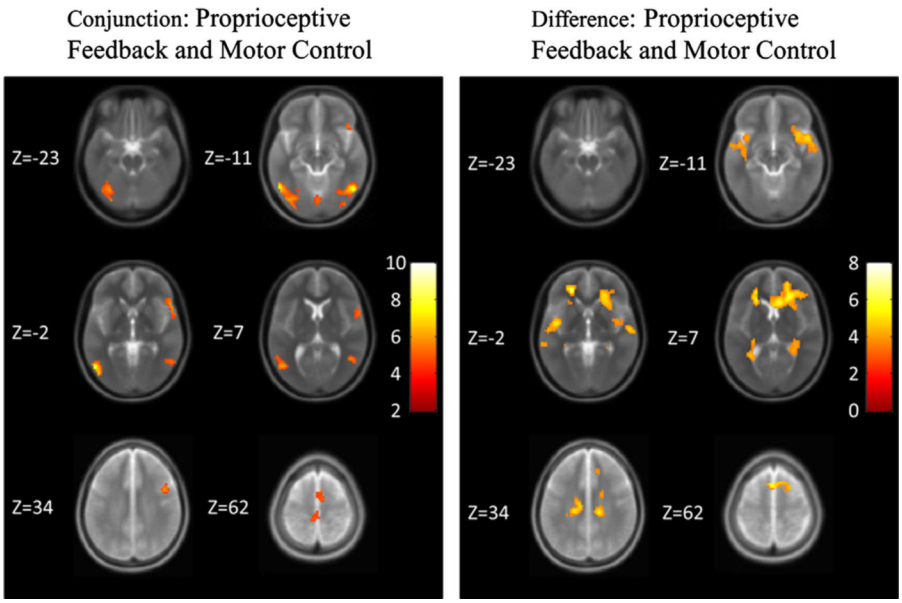

Fig. 3.

SPMs projected onto a normalized averaged structural (T2-weighted) image across six slices at significance $p<0.05$, AlphaSim corrected. Z values of the slices are given. The color bar shows the t-statistic (T-score). (Left) Areas that were activated during both the ankle DF/PF task vs. visual stimulation control task and the active balance simulation task vs. the visual stimulation control task. (Right) Areas that were activated during the active balance simulation task more greatly than the ankle DF/PF task.

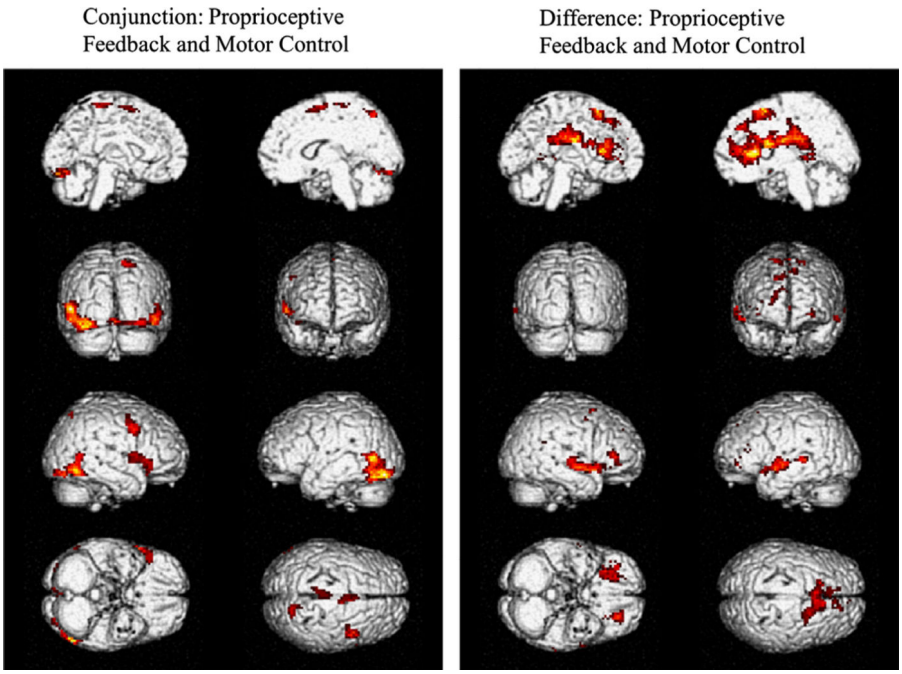

Fig. 4.

SPMs projected onto 3D rendered brains at significance $p<0.05$, AlphaSim corrected. (Left) Areas that were activated during both the ankle DF/PF task vs. visual stimulation control task and the active balance simulation task vs. visual stimulation control task. (Right) Areas that were activated during the active balance simulation task more strongly than ankle DF/PF task. The ankle DF/PF task showed no areas of activation that were greater than the active balance simulation task at significance $p<0.05$, AlphaSim corrected.

Table 1

Movement	Interscan		Intrascan	
	Mean ± std	Range	Mean ± std	Range
X translation (mm)	0.8 ± 0.4	[0.3–1.8]	0.1 ± 0.1	[0.0–0.4]
Y translation (mm)	0.8 ± 0.5	[0.3–1.9]	0.2 ± 0.1	[0.1–0.6]
Z translation (mm)	1.7 ± 0.6	[0.7–2.6]	0.3 ± 0.1	[0.1–0.5]
Total translation	2.0 ± 0.8	[0.8–3.7]	0.4 ± 0.2	[0.1–1.0]
X rotation (deg)	1.6 ± 0.6	[0.8–2.7]	0.3 ± 0.2	[0.1–0.9]
Y rotation (deg)	0.7 ± 0.5	[0.3–1.8]	0.1 ± 0.1	[0.1–0.6]
Z rotation (deg)	0.8 ± 0.4	[0.3–1.8]	0.2 ± 0.1	[0.1–0.3]

Table 2

Area	BA	Right hemisphere					Left hemisphere				
		T-value	*X*	*Y*	*Z*	Cluster	*T*-value	*X*	*Y*	*Z*	Cluster
Fusiform gyrus	BA 37						5.4	–42	–64	–17	370
Fusiform gyrus	BA 19						5.0	–33	–82	–20	
Middle temporal gyrus							4.9	–51	–64	–2	
Fusiform gyrus		8.0	48	–61	–17	171					
Middle temporal gyrus		4.9	48	–55	7						
Temporal lobe, subgyral		4.2	45	–64	–5						
Inferior frontal gyrus		6.4	51	26	–5	105					
Inferior frontal Gyrus	BA 47	5.9	45	26	–11						
Precentral gyrus	BA 44	4.2	57	11	10						
Middle frontal gyrus	BA 9	7.6	48	8	37	87					
Middle frontal gyrus		7.2	39	2	52						
Superior frontal gyrus	BA 6	6.5	3	11	58	47					

Table 3

Area	BA	Right hemisphere					Left hemisphere				
		T-value	*X*	*Y*	*Z*	Cluster	*T*-value	*X*	*Y*	*Z*	Cluster
Corpus callosum		7.4	6	23	10	2690					
Corpus callosum		5.6	24	32	7						
Caudate		5.3	12	6	14						
Superior frontal gyrus	BA 6						5.5	–3	16	55	
Medial frontal gyrus							5.4	–21	42	–6	
Middle frontal gyrus							6.2	–24	41	–2	
Anterior cingulate							4.9	–15	29	19	
Superior temporal gyrus	BA 22						5.0	–45	–4	–5	201
Middle temporal gyrus							4.0	–54	–13	–5	
Inferior frontal gyrus							3.9	–36	14	–14	
Sublobar, extra-nuclear							4.7	–33	–52	4	73
Sublobar, extra-nuclear							3.9	–27	–31	4	
Middle temporal gyrus	BA 22						3.9	–63	–34	1	42
Superior temporal gyrus							3.6	–45	–40	4	
Superior temporal gyrus							3.3	–57	–25	1	
Insula		4.0	39	–10	16	35					
Insula		3.6	45	–22	22						